Supersymmetric phases, the electron electric dipole moment and the muon magnetic moment

R. Arnowitt, B. Dutta, and Y. Santoso
Center For Theoretical Physics, Department of Physics, Texas A&M University, College Station, Texas 77843-4242
(Received 28 June 2001; published 8 November 2001)

The electron electric dipole moment (d_e) and the muon magnetic moment anomaly (a_μ) recently observed at BNL are analyzed within the framework of SUGRA models with CP violating phases at the GUT scale. It is seen analytically that even if d_e were zero, there can be a large B-ino mass phase (ranging from 0 to 2π) with a corresponding large B soft breaking mass phase (of size $\lesssim 0.5$ with the sign fixed by the experimental sign of a_μ). The dependence of the B phase on the other SUSY parameters, the gaugino mass $m_{1/2}$, $\tan\beta$, A_0, is examined. The lower bound of a_μ determines the upper bound of $m_{1/2}$. It is shown analytically how the existence of a nonzero B-ino phase reduces this upper bound (which would correspondingly lower the SUSY mass spectra). The experimental upper bound on d_e determines the range of allowed phases, and the question of whether the current bound on d_e requires any fine-tuning is investigated. At the electroweak scale, the phases have to be specified to within a few percent. At the GUT scale, however, the B phase requires fine-tuning below the 1% level over parts of the parameter space for low $m_{1/2}$, and if the current experimental bound on d_e were reduced by only a factor of 3–4, fine-tuning below 1% would occur at both the electroweak and GUT scales over large regions of the parameter space. All accelerator constraints ($m_h > 114$ GeV, $b \to s\gamma$, etc.) and relic density constraints with all stau-neutralino coannihilation processes are included in the analysis.

DOI: 10.1103/PhysRevD.64.113010 PACS number(s): 14.60.Ef, 04.65.+e, 11.30.Er, 14.80.Ly

I. INTRODUCTION

The role that CP violation plays in elementary particle physics and how it relates to current theory still remains after many years unclear. In the standard model (SM), CP violation is accommodated by inserting a single phase into the Cabibbo-Kobayashi-Maskawa (CKM) matrix, and there are now under way a number of experiments to test the validity of this idea [1]. In supersymmetry, the CKM phase can also exist, but it is possible to have additional phases appearing in the soft breaking masses. From the viewpoint of string theory, CP violating phases are a natural occurrence. Thus in 10 or 11 dimensional M-theory models with six dimensions compactified on a Calabi-Yau manifold, the Kähler potential and Yukawa matrices are represented by integrals over the Calabi-Yau space, and since this is a complex manifold, it is not surprising that CP violating phases can arise. With supersymmetry breaking, phases could arise also in the soft breaking masses. However, M-theory is not sufficiently developed to determine the details of such effects, and it is useful to have phenomenological constraints as a guide to where the fundamental theory may be.

As is well known, the existance of CP violating phases in the supersymmetric (SUSY) soft breaking masses leads to electric dipole moments (EDMs) for the electron and neutron, and the smallness of the current experimental bounds on these puts severe constraints on the parameter space. One may satisfy these constraints by assuming that the phases are nonzero but small [i.e., $O(10^{-2})$] or that the SUSY masses are large [i.e., $\gtrsim O(1\ \text{TeV})$]. The electron EDM (EEDM) arises from two diagrams: one involving the chargino-sneutrino intermediate state, and one involving the neutralino- selectron intermediate state. More recently it was suggested that a cancellation might occur between these two for relatively large phases [i.e., $O(10^{-1})$] over a reasonably large range of parameters [2], and there has been a large number of analyses based on this idea [3–6]. Diagrams similar to the above also enter into the muon $g-2$, and the recently reported 2.6σ deviation from the standard model value for that quantity [7] has placed significant bounds (at the 95% C.L.) on the allowed supergravity (SUGRA) parameter space [8]. It is thus natural to ask whether both constraints can be phenomenologically realized, and initial discussions of this have been made [9].

The minimal supersymmetric standard model (MSSM) has over 40 independent phases, and so cannot make significant theoretical predictions on this question. We use here instead supergravity (SUGRA) grand unified theory (GUT) models with gravity mediated supersymmetry breaking [10] and R-parity invariance.[1] Such models have become quite predictive, in part due to the fact that they automatically include the CERN e^+e^- collider LEP results on grand unification, and because radiative breaking of $SU(2)\times U(1)$ implies that the SUSY soft breaking masses are of electroweak size. Thus the general size of both $g-2$ and the EDMs (which depend on the size of the SUSY masses) are restricted. In addition, such models have a natural candidate for dark matter, the lightest neutralino ($\tilde{\chi}_1^0$), and the condition that the relic density of neutralinos be in accord with the allowed range from astronomical measurements also puts important constraints on the parameter space.

Previous analyses of the EDMs within the framework of SUGRA GUT models has shown that a new fine tuning prob-

[1]Two alternate SUGRA models are anomaly mediated [11] and gauge mediated [12] soft breaking. The former appears to have difficulty in satisfying the Brookhaven E821 bounds on $g-2$ when no SUSY CP phases are present [13], while the latter does not appear to have a satisfactory dark matter candidate [14].

lem arises at the GUT scale for θ_{B_0} (the phase of B, the bilinear soft breaking mass) when $\tan\beta$ gets large [4]. Further, the discussion of the muon $g-2$ have shown that $\tan\beta$ is greater than 5 (and very possibly greater than 10). In carrying out our analysis, then, we put a constraint on the parameter space that $\Delta\theta_{B_0}/\theta_{B_0}>0.01$, where $\Delta\theta_{B_0}$ is the allowed range that will satisfy the experimental bounds on the EDMs. In order to carry out a complete analysis, however, it is necessary to include all the accelerator constraints [i.e., that $m_h>114$ GeV (where h is the light Higgs boson), the CLEO bound on the $b\to s\gamma$ decay, etc.] as well as the full analysis of the relic density including all the stau-neutralino coannihilation channels. (The details of these were discussed in [15,16].)

Both the electron EDM and the muon $g-2$ can be calculated from two types of diagrams, one with the intermediate chargino and sneutrinos states, and one with the intermediate neutralino and slepton states. If one assumes universal soft breaking in the first two generations, then the EEDM and the SUSY deviation of the muon magnetic moment from its standard model value, $a_\mu^{\rm SUSY}$ ($a_\mu=(g_\mu-2)/2$), can both be calculated from a single amplitude for these diagrams, the former being related to the imaginary part, and the latter to the real part. In the following we will use the symbol a_μ to mean the deviation of the muon $(g_\mu-2)/2$ from its standard model value.

As is well known, for large $\tan\beta$, a_μ is dominated by the chargino diagram [17,18] (the neutralino diagrams being generally quite small), while the strong experimental constraints on the EEDM require a near cancellation between the neutralino and chargino diagrams [2]. In order to see how this can come about when CP violating phases are present, we calculate in the Appendix the leading large $\tan\beta$ terms. We discuss analytically in Sec. II how both experimental constraints can naturally be satisfied at the electroweak scale. In Sec. III we examine in detail numerically the combined experimental constraints of the EEDM and the Brookhaven E821 a_μ experiment on the SUSY parameter space for a variant of the MSUGRA model where the magnitudes of the soft breaking masses are universal at M_G but the phases are arbitrary. The experimental lower bound on a_μ puts an upper bound on the gaugino mass $m_{1/2}$, and this upper bound is generally reduced when CP violating phases are present. The Higgs boson mass lower bound and the $b\to s\gamma$ constraint generally put a lower bound on $m_{1/2}$. Imposing the fine tuning constraint at $M_{\rm GUT}$ generally increases that bound when CP violating phases are present and also limits the range of the CP violating phases. Thus the two experiments interact to further restrict the SUSY parameter space when CP violating phases are large. In Sec. IV we give some concluding remarks.

II. MUON MAGNETIC MOMENT AND ELECTRON EDM

We consider here supergravity models which are a generalization of minimal SUGRA (MSUGRA) to include the possibility of phases in the soft breaking masses at the GUT scale $M_G\cong 2\times 10^{16}$ GeV. The magnitude of the soft breaking masses are still assumed to be universal, but phases are not necessarily universal. Thus the SUSY parameters at M_G are m_0 (the scalar soft breaking mass), $m_{1/2i}=|m_{1/2}|\exp(i\phi_i)$ $i=1,2,3$ [the gaugino masses for the $U(1),SU(2),SU(3)$ groups], $A_0=|A_0|\exp(i\alpha_0)$ (cubic soft breaking mass), $B_0=|B_0|\exp(i\theta_{B_0})$ (quadratic soft breaking mass), and $\mu_0=|\mu_0|\exp(i\theta_\mu)$ (the Higgs mixing parameter in the superpotential). The model therefore depends on five magnitudes and six phases. However, one can always set one of the gaugino phases to zero, and we chose here $\phi_2=0$.

The renormalization group equations (RGEs) allow one to evaluate the parameters at the electroweak scale. To one loop order, the ϕ_i and θ_μ do not run. Further, radiative breaking of $SU(2)\times U(1)$ at the electroweak scale allows one to eliminate θ_μ in terms of θ_B, the B phase at the electroweak scale, and determine $|\mu|$ and $|B|$ in terms of the other parameters and $\tan\beta=|\langle H_2\rangle/\langle H_1\rangle|$. Thus with a convenient choice of Higgs VEV phases, the minimization of the Higgs potential yields [19]

$$\theta_\mu=-\theta_B+f(-\theta_B+\alpha_q,-\theta_B+\alpha_l) \tag{1}$$

$$|\mu|^2=\frac{m_1^2-\tan^2\beta m_2^2}{\tan^2\beta-1};\quad |B|=\frac{1}{2}\sin 2\beta\frac{m_3^2}{|\mu|} \tag{2}$$

where α_q and α_l are the quark and lepton phase of A_q and A_l at the electroweak scale, $m_i^2=m_{H_i}^2+\Sigma_i$ $(i=1,2)$, $m_3^2=2|\mu|^2+m_1^2+m_2^2$, and m_{H_i} are the Higgs boson running masses at the electroweak scale. $\Sigma_i=dV_1/dv_i^2$ where V_1 is the one loop contribution to the Higgs potential, and $v_i=|\langle H_i\rangle|$. There remain therefore four real parameters which we take to be m_0, $|A_0|$, $|m_{1/2}|$, and $\tan\beta$, and four phases θ_{B_0}, α_0, ϕ_1, and ϕ_3. In this paper we examine only the electron electric dipole moment[2] (EEDM), and so our results are only very weakly dependent on ϕ_3. Also, since we are dealing only with first and second generation sleptons, there is only a weak dependence on α_0. Thus the two important phases are θ_{B_0} and ϕ_1. The parameter range that we examine is

$$|m_0|<1\ \text{TeV};\quad |m_{1/2}|<1\ \text{TeV};\quad |A_0/m_{1/2}|<4 \tag{3}$$

$$\tan\beta\leqslant 40. \tag{4}$$

As discussed above, both a_μ and d_e can be obtained from the same complex amplitude A (assuming universal soft breaking in the first two generations). One has then

[2]While there has been considerable progress in calculating the neutron EDM [20] and ^{199}Hg EDM [5], there remain still significant hadronic uncertainties, in contrast to the clear calculation of the EEDM. Further, the ϕ_3 phase can always be adjusted to satisfy the neutron EDM, and the effect of the ^{199}Hg EDM would then only result in reducing the remaining parameter space that we find from the EEDM and the muon $g-2$ given here.

$$a_\mu = -\frac{\alpha}{4\pi \sin^2\theta_W} m_\mu^2 \ \mathrm{Re}[A] \tag{5}$$

$$d_e/e = -\frac{\alpha}{8\pi \sin^2\theta_W} m_e \ \mathrm{Im}[A]. \tag{6}$$

The amplitude A is defined in the Appendix. For the case where there are no CP violating phases, the experimental a_μ data [7] favors large $\tan\beta$ [8]. In order to see semiquantitatively the nature of the cancellations needed to make d_e small, the leading terms for large $\tan\beta$ were obtained in the Appendix when $\mu^2 \gg M_W^2$ (which is almost always the case for the MSUGRA parameter space). From Eqs. (A18), (A25) we find for the neutralino and chargino diagrams

$$a_\mu = a(\tilde{\chi}^\pm) + a(\tilde{\chi}^0) \tag{7}$$

where

$$a(\tilde{\chi}^\pm) = C_\mu(\tilde{\chi}^\pm)\left[\frac{|\mu|^2}{|\mu|^2-\tilde{m}_2^2}F_1 - \frac{\tilde{m}_2^2}{|\mu|^2-\tilde{m}_2^2}F_2\right]\cos\theta_\mu \tag{8}$$

$$\begin{aligned} a(\tilde{\chi}^0) = C_\mu(\tilde{\chi}^0)\Bigg[&\Bigg\{\left(\frac{|\mu|^2}{m^2_{\tilde{u}_L}-m^2_{\tilde{u}_R}} - \frac{|\mu|^2}{|\mu|^2-\tilde{m}_1^2}\right)G_{11} \\ &-\left(\frac{|\mu|^2}{m^2_{\tilde{u}_L}-m^2_{\tilde{u}_R}} - \frac{1}{2}\frac{|\mu|^2}{|\mu|^2-\tilde{m}_1^2}\right)G_{21}\Bigg\} \\ &\times\cos(\theta_\mu+\phi_1) - \frac{1}{2\tan^2\theta_W}\frac{|\tilde{m}_1|}{\tilde{m}_2}\frac{|\mu|^2}{|\mu|^2-\tilde{m}_2^2} \\ &\times\Bigg\{\left(G_{22} - \frac{1}{2}\left(\frac{\tilde{m}_2}{|\mu|}\right)^2 G_{23}\right) \\ &\times\cos\theta_\mu - \frac{1}{2}\frac{\tilde{m}_2}{|\mu|}G_{23}\Bigg\}\Bigg] \end{aligned} \tag{9}$$

where

$$C_\mu(\tilde{\chi}^\pm) = \frac{\alpha\, m_\mu^2 \tan\beta}{4\pi\tilde{m}_2|\mu|\sin^2\theta_W} \tag{10}$$

and $C_\mu(\tilde{\chi}^0) = \tan^2\theta_W(\tilde{m}_2/|\tilde{m}_1|)C_\mu(\tilde{\chi}^\pm)$. The form factors $F_i = F(m^2_{\tilde{\nu}}/m^2_{\tilde{\chi}_i^\pm})$ and $G_{ki} = G(m^2_{\tilde{\mu}_k}/m^2_{\tilde{\chi}_i^0})$ are defined in Eqs. (A8),(A12), and $|\tilde{m}_1| \cong 0.4 m_{1/2}$, $\tilde{m}_2 \cong 0.8 m_{1/2}$. (Our states are labeled such that e.g., $m_{\tilde{\chi}_i^0} < m_{\tilde{\chi}_j^0}$ for $i<j$.)

A similar decomposition of the electron electric dipole moment, $d_e/e = d(\tilde{\chi}^\pm) + d(\tilde{\chi}^0)$, gives

$$d(\tilde{\chi}^\pm) = -D_e(\tilde{\chi}^\pm)\left[\frac{|\mu|^2}{|\mu|^2-\tilde{m}_2^2}F_1 - \frac{\tilde{m}_2^2}{|\mu|^2-\tilde{m}_2^2}F_2\right]\sin\theta_\mu \tag{11}$$

$$\begin{aligned} d(\tilde{\chi}^0) = -D_e(\tilde{\chi}^0)\Bigg[&\Bigg\{\left(\frac{|\mu|^2}{m^2_{\tilde{u}_L}-m^2_{\tilde{u}_R}} - \frac{|\mu|^2}{|\mu|^2-\tilde{m}_1^2}\right)G_{11} \\ &-\left(\frac{|\mu|^2}{m^2_{\tilde{u}_L}-m^2_{\tilde{u}_R}} - \frac{1}{2}\frac{|\mu|^2}{|\mu|^2-\tilde{m}_1^2}\right)G_{21}\Bigg\}\sin(\theta_\mu+\phi_1) \\ &-\frac{1}{2\tan^2\theta_W}\frac{|\tilde{m}_1|}{\tilde{m}_2}\frac{|\mu|^2}{|\mu|^2-\tilde{m}_2^2} \\ &\times\left(G_{22} - \frac{1}{2}\left(\frac{\tilde{m}_2}{|\mu|}\right)^2 G_{23}\right)\sin\theta_\mu\Bigg] \end{aligned} \tag{12}$$

where $D_e = (m_e/2m_\mu^2)C_\mu$.

In the case where all phases are zero, it is well known that the chargino contribution to a_μ dominates over the neutralino diagram even though the front factors $C_\mu(\tilde{\chi}^\pm)$ and $C_\mu(\chi^0)$ are of comparable size. This can be understood from Eqs. (8) and (9) in the following way. The second term in Eq. (8), coming from the heavy chargino, $\tilde{\chi}_2^\pm$, cancels about 30% of the light chargino contribution. In a similar fashion, the second term in Eq. (10) coming from the heavy smuon, $\tilde{\mu}_2$, contribution cancels part of the leading term. However, due to the slowly varying nature of the form factors G_{11} and G_{21}, about 75% of the leading G_{11} term is canceled, reducing $a(\tilde{\chi}^0)$ significantly. The remaining two terms arising from the heavy neutralinos, $\tilde{\chi}^0_{2,3,4}$ are generally small (and there can be cancellations also between these terms). In contrast, when the CP violating phases are not zero and an electric dipole moment exits, the neutralino and chargino contributions must be of nearly equal size and opposite sign so that d_e be greatly suppressed to be in accord with experiment. This change in the relative sizes of the two terms must be brought about by the sine factors in Eqs. (11),(12). Simultaneously, the corresponding cosine factors in Eqs. (8), (9) will modify the predictions of a_μ. This then leads to two questions: (1) Can the experimental constraints on d_e and a_μ (and of course all other experimental constraints) be simultaneously satisfied with "large" phases, i.e., of $O(10^{-1})$? (2) If large phases are possible (and d_e is very small) can the experimental constraints be satisfied without undue fine-tuning of the phases? Question (2) divides into two parts: (2a) Is there undue fine-tuning of phases needed to satisfy the experimental constraints at the electroweak scale, and (2b) Is there undue fine-tuning of the phases needed at the GUT scale? In the following, we define the fine tuning parameter $R(\phi)$ for any phase ϕ by

$$R(\phi) \equiv \frac{\phi_2 - \phi_1}{\frac{1}{2}(\phi_2+\phi_1)} \equiv \frac{\Delta\phi}{\phi_{\mathrm{av}}} \tag{13}$$

where ϕ_2 and ϕ_1 are the upper and lower value of ϕ when the experimental constraints on d_e and a_μ are both satisfied. We use here the current bound on d_e [21],

$$|d_e| < 4.3\times 10^{-27} e \ \text{cm} \tag{14}$$

and the 2 std range for a_μ [7]:

$$11\times 10^{-10} < a_\mu < 75\times 10^{-10}. \tag{15}$$

In the following we will assume that no fine-tuning less than 1% be allowed: i.e.,

$$R(\phi) > 0.01. \tag{16}$$

Within this framework, we find that question (1) can be answered affirmatively, i.e., cancellations between the neutralino and chargino diagrams in d_e can indeed be satisfied with large phases. Further, the answer to question 2(a) is that no undue fine-tuning of the electroweak parameters is necessary to achieve the suppression of d_e. However, we will see that this is not the case at the GUT scale, where the simultaneous requirements of electroweak radiative breaking and the experimental d_e constraint leads to significant fine-tuning, and if Eq. (16) were imposed, a large amount of the parameter space is eliminated.

In a GUT theory, the fundamental parameters are specified at $M_{\rm GUT}$, and the consequences at the electroweak scale are obtained from the renormalization group equations (RGEs). These GUT parameters are presumably to be determined at some future time by a more fundamental theory (e.g., string theory), and so fine tuning at the GUT scale may imply a significant theoretical problem (while fine-tuning at the electroweak scale would be an acceptable theoretical consequence of the RGEs). Of course, what level of fine tuning is acceptable is somewhat a matter of choice, and we view Eq. (16) only as a reasonable benchmark to consider.

In Sec. III below, we will consider these results in detail quantitatively. We give here an analytic discussion of how they arise. To show that large phases are easily achievable, we write d_e in the form

$$d_e/e = -D_e(\tilde{\chi}^{\pm})A[\sin(\theta_\mu) + a\sin(\theta_\mu + \phi_1)] \tag{17}$$

where the coefficients A and a can be read off from Eqs. (11), (12). In the extreme case where $d_e = 0$, Eq. (17) and Eq. (1) imply

$$\tan\theta_B = \frac{a\sin\phi_1}{1 + a\cos\phi_1} \tag{18}$$

where we have neglected the small 1-loop correction in Eq. (1). The fact that the chargino diagram dominates over the neutralino diagram implies that $a < 1$, and detailed numerical calculations show that $a \sim 0.2$–0.4 for much of the SUSY parameter space. Thus as ϕ_1 varies from 0 to 2π, over most of the parameter space $|\theta_B|$ will be large (rising to a maximum of about 0.5) even though d_e has been set to zero.

We next consider the effects of the CP violating phases on a_μ. From Eqs. (8),(9), we have

$$a_\mu = C_\mu(\tilde{\chi}^{\pm})A[\cos(\theta_\mu) + a\cos(\theta_\mu + \phi_1) + b] \tag{19}$$

where b is the term in Eq. (9) independent of the phases. In general, b is quite small, and we will neglect it in the following. (Of course, in the numerical calculations in Sec. III all such effects as well as the loop corrections are considered.) Using Eq. (18) to eliminate θ_B, we obtain

$$a_\mu = \pm a_\mu(0) Q(a, \phi_1) \tag{20}$$

where $a_\mu(0)$ is the value of a_μ with zero phases,

$$Q = \frac{[1 + 2a\cos\phi_1 + a^2]^{1/2}}{(1+a)} \leqslant 1. \tag{21}$$

The $\pm$ factor in Eq. (20) is the sign of $\cos\theta_B$. Since experimentally, $a_\mu > 0$, this implies

$$\theta_B > 0 \quad \text{for} \quad 0 < \phi_1 < \pi; \quad \theta_B < 0 \quad \text{for} \quad \pi < \phi_1 < 2\pi. \tag{22}$$

The two branches of Eq. (22) are symmetric, and in the following we consider the $\theta_B > 0$ branch. The factor Q in Eq. (21) reduces the theoretically expected size for a_μ. Since the experimental lower bound on a_μ implies an upper bound on $m_{1/2}$ [8], the Q factor due to the phases will reduce this upper bound, further restricting the allowed SUSY parameter space. However, since in general $Q \gtrsim 0.5$, this reduction will still be consistent with all experimental data, and the effect of the SUSY CP violating phases does not qualitatively change the fit to the data for a_μ that was obtained assuming no CP violating phases.

We can also estimate how much fine tuning is needed in the phases to satisfy the experimental bound of Eq. (14). Thus let $\Delta\theta_B$ be the change in θ_B for a fixed value of ϕ_1 as d_e/e varies from -4.3×10^{-27} cm to $+4.3\times 10^{-27}$ cm. Characteristically, the factor $D(\tilde{\chi}^{\pm})A$ in Eq. (17) is numerically about 100 times the current upper bound on d_e [e.g., for $m_{1/2} = 480$ GeV ($m_0 = 118$ GeV), $|\mu| = 690$ GeV, and $\tan\beta = 15$, this factor is 4.1×10^{-25} cm]. Considering then the variation of θ_B in Eq. (17) one finds

$$2\times 10^{-2} \cong \Delta\theta_B \cos(\theta_B)[1 + a\cos(\phi_1) + a\sin(\phi_1)\tan(\theta_B)]. \tag{23}$$

Hence using Eq. (18),

$$R(\theta_B) \cong \Delta\theta_B/\sin(\theta_B) \cong 2\times 10^{-2}/(a\sin(\phi_1)). \tag{24}$$

Thus the allowed range of θ_B is indeed small, though the condition of Eq. (16) is generally satisfied. A reduction of d_e by a factor of 10 would be enough to produce a serious fine-tuning problem at the electroweak scale. In contrast, we will see below that there is already a significant fine-tuning problem at the GUT scale even with the current bound on d_e.

III. DETAILED CALCULATIONS

In this section, we consider detailed calculations of the effects of the experimental constraints involving the EEDM and a_μ which were analytically estimated in Sec. II. The analysis is done within the framework of the generalized

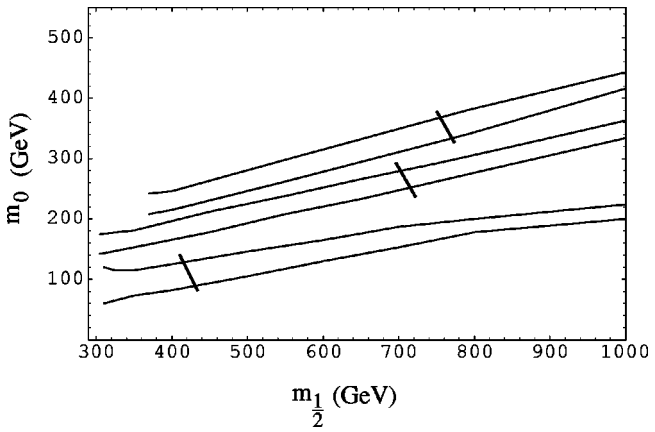

FIG. 1. Corridors in the $m_0-m_{1/2}$ plane allowed by the relic density constraint for (bottom to top) $\tan\beta=10,30,40$ for $m_h>114$ GeV, $A_0=0$, $\mu>0$, all phases set to zero. The $\tan\beta=30$ and 40 corridors all lie in the coannihilation region, while only the beginning of the $\tan\beta=10$ corridor is in the noncoannihilation region. The Higgs boson mass bound determines the lower $m_{1/2}$ bound for $\tan\beta=10$, while both the Higgs boson mass and the $b\to s\gamma$ bounds equally produce the lower bound for $\tan\beta=30$ and $b\to s\gamma$ determines the lower bound for $\tan\beta=40$. The short slanted lines represent the upper bound on $m_{1/2}$ due to the a_μ lower bound, of Eq. (15).

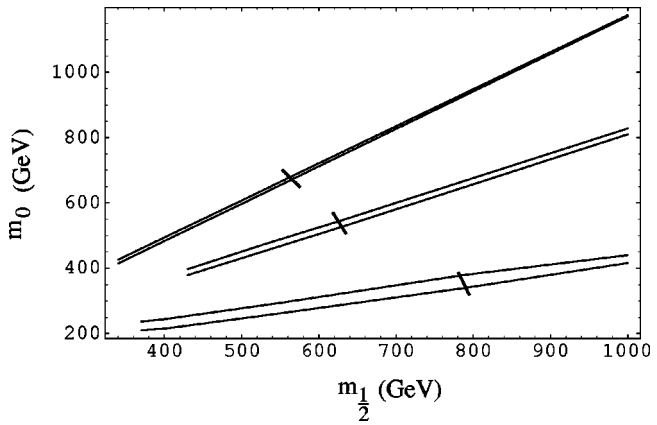

FIG. 2. Corridors in the $m_0-m_{1/2}$ plane allowed by the relic density constraint for (from bottom to top) $A_0=0$, $-2m_{1/2}$, $4m_{1/2}$, for $m_h>114$ GeV, $\mu>0$, all phases set to zero. The lower $m_{1/2}$ bounds for $A_0=0$, $-2m_{1/2}$ are due to the $b\to s\gamma$ constraint, and for $A_0=4m_{1/2}$ from the Higgs boson mass bound [15].

MSUGRA described in Sec. II (though extension to nonuniversal soft breaking models can easily be done). In order to get a clear picture of what constraints on the SUSY parameter space arise, it is necessary to simultaneously impose all the experimental constraints. Aside from the above, these include the following: (1) The LEP Higgs boson mass lower bound $m_h>114$ GeV [22]. Since the theoretical analysis of m_h still has about a 3 GeV uncertainty [which (conservatively) may be an overestimate] we interpret this in the theoretical calculation [15] to mean $m_h>111$ GeV. (2) The $b\to s\gamma$ branching ratio constraint. We take here a 2 std range of the experimental CLEO data [23]

$$1.8\times10^{-4}\leqslant BR(B\to X_s\gamma)\leqslant 4.5\times10^{-4}. \tag{25}$$

In the theoretical analysis we include the next leading order (NLO) SUSY contribution for large $\tan\beta$ [24], as these produce significant effects (particularly since the a_μ lower bound favors larger values of $\tan\beta$). (4) We include the 1-loop corrections to the b and τ masses [25], which are significant also for large $\tan\beta$. (5) All coannihilation effects are included in the relic density calculations. We assume here the range for the neutralino cold dark matter to be

$$0.025<\Omega_{\tilde\chi_1^0}h^2<0.25. \tag{26}$$

The upper bound is consistent with recent Boomerang and Maxima measurements [26,27], while the lower bound allows for the possibility that there may be more than one type of dark matter. However, our calculations here are insensitive to the precise value of the lower bound, and one would get very similar results if the lower bound were raised to 0.05 or 0.1.

The effects of the Higgs boson mass and $b\to s\gamma$ bounds is to push the allowed parameter space mostly into the coannihilation domain of the relic density calculation. (Thus only a small part of the allowed parameter space occurs at small enough $m_{1/2}$ to lie below the region of coannihilation, which begins at $m_{1/2}\cong 350-400$ GeV.) In SUGRA models, stau-neutralino coannihilation can occur quite naturally. Thus for $m_0=0$, the charged sleptons lie below the lightest neutralino, $\tilde\chi_1^0$, and one must increase m_0 to raise their masses so that the $\tilde\chi_1^0$ is the dark matter particle. Thus as $m_{1/2}$ increases, m_0 must be increased in lock step so that the neutralino remains the lightest supersymmetric particle (LSP), and one finds a relatively narrow corridor in the $m_0-m_{1/2}$ plane consistent with the relic density bound of Eq. (26) and with the lightest stau lying above the neutralino. The dependence of these corridors on $\tan\beta$ and A_0 are shown in Figs. 1 and 2 for the case where there are no SUSY CP violating phases. We see that the corridors (which are characteristically 20–30 GeV wide) lie higher for larger $\tan\beta$ and larger $|A_0|$. This is because the stau mass decreases when these parameters are increased, and so one must raise m_0 to keep the stau mass greater than the neutralino.[3] In general, the effect of coannihilation is to determine m_0 approximately in terms of $m_{1/2}$ for a given $\tan\beta$ and A_0. This greatly sharpens the predictions of the theory.

A. Allowed regions at the electroweak scale for θ_B and ϕ_1

We now examine the effects of having nonzero CP violating phases present, and discuss the dependence of the allowed phases on the SUSY parameters. To illustrate the phenomena, we consider one low $\tan\beta$ and one high $\tan\beta$.

[3]Increasing $\tan\beta$ or making A_0 negative increases the magnitude of the LR term in the stau mass matrix of Eq. (A3) and hence decreases the light stau mass. For $A_0>0$, the opposite effect occurs, but also the diagonal matrix elements of the mass matrix are reduced, and again the stau mass decreases.

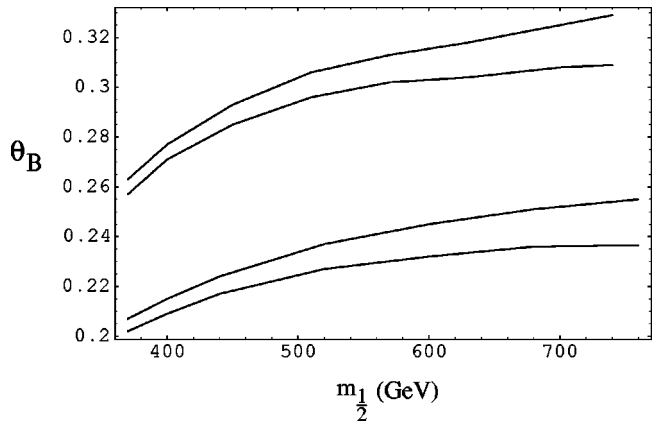

FIG. 3. Regions allowed for θ_B by the experimental constraint on d_e as a function of $m_{1/2}$ for $\tan\beta=40$, $A_0=0$, for $\phi_1=0.9$ (lower curves) and $\phi_1=1.2$ (upper curves).

Since for no CP violating phases, one had (at 90% C.L.) $\tan\beta>10$, we examine the cases of $\tan\beta=15$ and $\tan\beta=40$. Figure 3 shows the corridors allowed for θ_B (the B phase at the electroweak scale) by the current experimental bounds on d_e for $\tan\beta=40$, $A_0=0$ for two choices of the gaugino phase: $\phi_1=0.9$ (lower curves) and $\phi_1=1.2$ (upper curves). One sees that one gets a significant phase θ_B of the size expected by Eq. (18), the larger ϕ_1 allowing a larger θ_B, also in accord with Eq. (18). Note also that the allowed corridors for θ_B widens as $m_{1/2}$ increases as expected, since the experimental d_e constraint is less severe for a heavier mass spectrum. A similar graph is shown in Fig. 4 for $\phi_1=0.9$ (upper curves), $\phi_1=3.4$ (lower curves). θ_B turns negative for ϕ_1 in the third quadrant, again as expected from Eq. (22).

We note in all these curves, the upper bound on $m_{1/2}$ (due to the lower bound on a_μ) is reduced compared to the case when the CP violating phases are zero. (Then the upper bound is $m_{1/2}=790$ GeV for $\tan\beta=40$, $A_0=0$ [8].) This is due to the phase ϕ_1 in the Q factor in Eq. (20). Q is smallest when ϕ_1 is near π, as can be seen in explicitly in Fig. 4 for $\phi_1=3.4$.

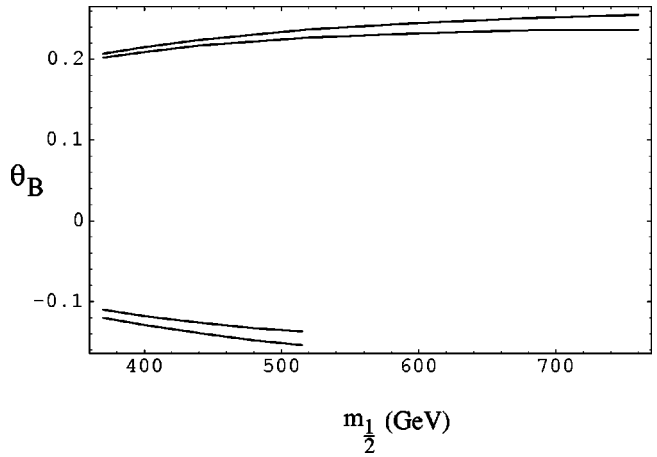

FIG. 4. Same as Fig. 3 for $\phi_1=0.9$ (upper curves) and $\phi_1=3.4$ (lower curves).

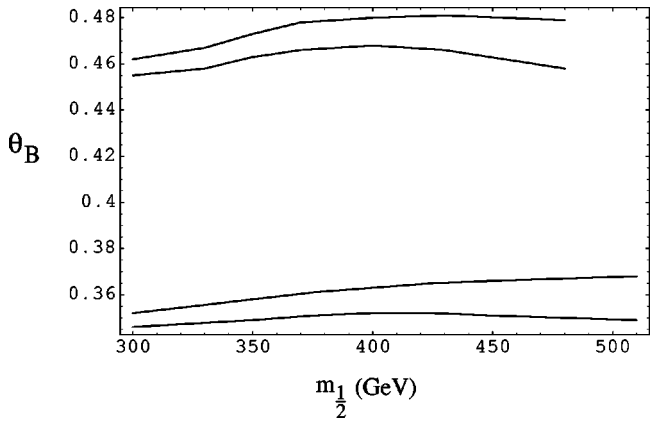

FIG. 5. Same as Fig. 3 for $\tan\beta=15$. The allowed regions terminate at low $m_{1/2}$ due to the m_h constraint.

We consider next the $\tan\beta$ dependence of the allowed region for θ_B. This arises due to an indirect $\tan\beta$ dependence in the parameter a of Eqs. (17),(18). As seen from Fig. 2, coannihilation determines m_0 in terms of $m_{1/2}$, and this m_0 increases with $\tan\beta$, changing the ratio of neutralino to chargino diagram differentially. Figure 5 shows the allowed region for $\tan\beta=15$, and $A_0=0$, $\phi_1=1.2$ (upper curves) and $\phi_1=0.9$ (lower curves). We see that one can get considerably larger values of θ_B at lower $\tan\beta$, though the upper bound on $m_{1/2}$ due to the lower bound on a_μ is considerably reduced at low $\tan\beta$. The A_0 dependence is exhibited in Fig. 6, where the allowed corridor for θ_B is plotted for $\tan\beta=40$, $\phi_1=0.9$, and $A_0=0$ (upper curves), $|A_0|=2m_{1/2}$, $\alpha_0=0.5$ (lower curves). Increasing the magnitude of A_0 increases the value of m_0 (by Fig. 2) and reduces the size of θ_B.

B. Fine tuning at the electroweak scale

The above analysis shows that the d_e experimental constraint allows θ_B to be $O(10^{-1})$ for a wide region of parameter space, and ϕ_1 can range widely, i.e., from 0 to 2π. We next investigate whether the smallness of the upper bound on d_e requires any fine tuning to maintain this constraint. In Fig. 7 we plot the fine tuning parameter R of Eq. (13) for θ_B for

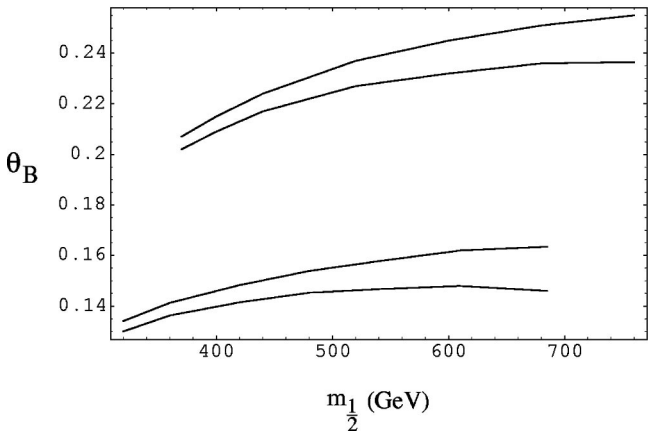

FIG. 6. Allowed region for θ_B for $\tan\beta=40$ for $A_0=0$ (upper curves) and $|A_0|=2m_{1/2}$, $\alpha_0=0.5$ (lower curves).

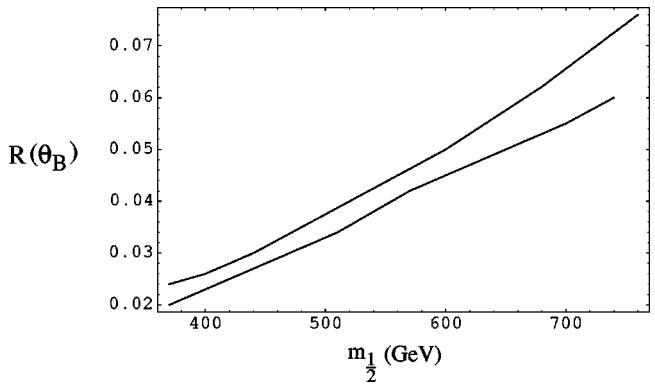

FIG. 7. $R(\theta_B)$ as a function of $m_{1/2}$ for $\tan\beta=40$, $A_0=0$, $\phi_1=0.9$ (upper curve), $\phi_1=1.2$ (lower curve).

$\tan\beta=40$, $A_0=0$ for $\phi_1=0.9$ (upper curve) and $\phi_1=1.2$ (lower curve). One sees that $R(\theta_B)$ is small, i.e., a few percent, but satisfies the criteria $R>0.01$ for the entire range. The size of $R(\theta_B)$ is consistent with what was expected from the analytic analysis of Eq. (24), and increases as ϕ_1 decreases also as expected. Figure 8 shows a similar plot for $\tan\beta=15$. Since θ_B is larger here (see Fig. 5), $R(\theta_B)$ is smaller, but still within the acceptable range. Figure 9 shows $R(\phi_1)$ for $\tan\beta=40$, $A_0=0$ for $\theta_B=0.2$ (upper curve), and $\theta_B=0.3$ (lower curve). Again $R(\phi_1)>0.01$ for the entire range of $m_{1/2}$, and is generally larger than $R(\theta_B)$ (by about a factor of $\tan\phi_1/\phi_1$).

We see from the above results that the current experimental bound on d_e can be accommodated with large phases. Further, for most of the parameter space, while the range of the allowed phases at the electroweak scale required to accommodate the bound on d_e is small, no fine-tuning below 1% is needed. We will see, however, a more serious fine-tuning problem develops at the GUT scale.

C. Fine tuning at the GUT scale

We now examine what parameters are fine tuned at the GUT scale to achieve the experimental EDM bounds. From Eq. (1), we see since the loop correction is small, that $\theta_\mu\cong-\theta_B$, and since we have seen that θ_B does not need excessive fine tuning, the same can be said for θ_μ. Further, since

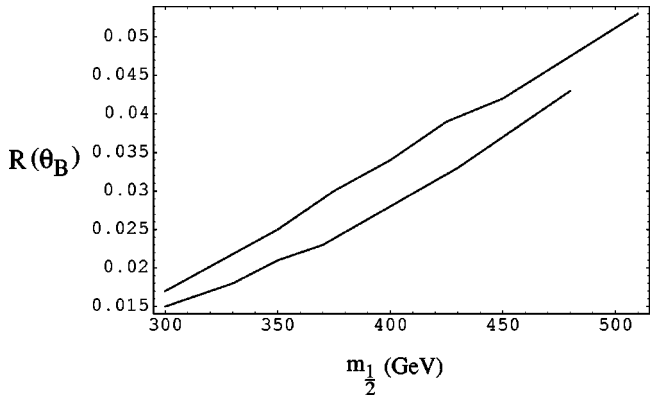

FIG. 8. Same as Fig. 7 for $\tan\beta=15$.

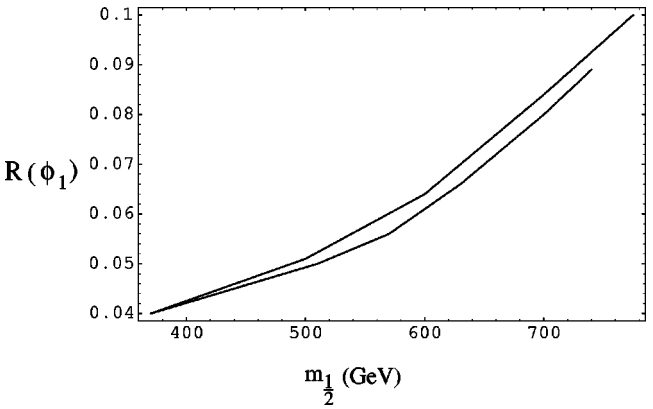

FIG. 9. $R(\phi_1)$ as a function of $m_{1/2}$ for $\tan\beta=40$, $A_0=0$, and $\theta_B=0.2$ (upper curve), $\theta_B=0.3$ (lower curve).

θ_μ does not run with the RGE, its value at the GUT scale is the same as at the electroweak scale and hence no fine tuning is needed at M_G. A similar result holds for ϕ_1, which also does not run with the RGE. However, as has been previously pointed out [4], matters are different for the B phase at M_G, θ_{B_0}, and we review briefly the discussion given there.[4] To see analytically what is occurring, we consider the intermediate and low $\tan\beta$ region, where the RGE can be analytically solved. One finds for B the result [4]

$$B=B_0-\frac{1}{2}(1-D_0)-\sum\ \Phi_i|m_{1/2}|e^{i\phi_i} \tag{27}$$

where $D_0=1-(m_t/\sin\beta)^2\lesssim 0.25$ and $\Phi_i=O(1)$. As $\tan\beta$ gets large, the radiative breaking condition Eq. (2) shows that $|B|$ gets small. Taking the imaginary part of Eq. (27) gives

$$|B|\sin\theta_B=|B_0|\sin\theta_{B_0}-(1/2)(1-D_0)|A_0|\sin\alpha_0$$

$$-\sum\ \Phi_i|m_{1/2}|\sin\phi_i\,. \tag{28}$$

To the lowest approximation, since $|B|$ is small, one may then neglect the left-hand side (LHS) of Eq. (28). Equation (28) may then be viewed as an equation determining θ_{B_0} in terms of the other GUT scale phases, and hence θ_{B_0} will in general be large if the other phases are not all small (a result that is confirmed in [4] by detailed calculation). However, the range of θ_{B_0} so that the experimental bound on d_e is satisfied is then significantly reduced. Thus for fixed values of α_0 and ϕ_i, Eq. (28) gives as $\tan\beta$ gets large (i.e., $|B|$ becomes small)

$$\Delta\theta_{B_0}\cong(|B|/|B_0|)\Delta\theta_B\ll\Delta\theta_B\,. \tag{29}$$

Since we have already seen that $\Delta\theta_B$ is small (though not violating the fine tuning condition), one may expect that

[4]This analysis differs from that given in [28] which does not take into account the possibility of cancellations in d_e between the neutralino and chargino diagrams. In fact the discussion in [28] sets the phase θ_{B_0} to zero.

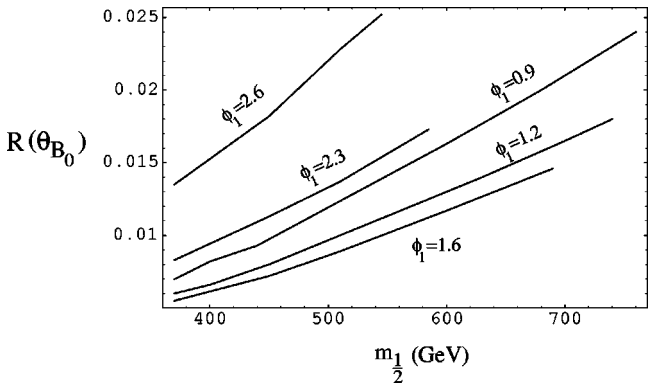

FIG. 10. $R(\theta_{B_0})$ as a function of $m_{1/2}$ for $\tan\beta=40$, $A_0=0$ for (from bottom to top) $\phi_1=1.6$, 1.2, 0.9, 2.3 and 2.6.

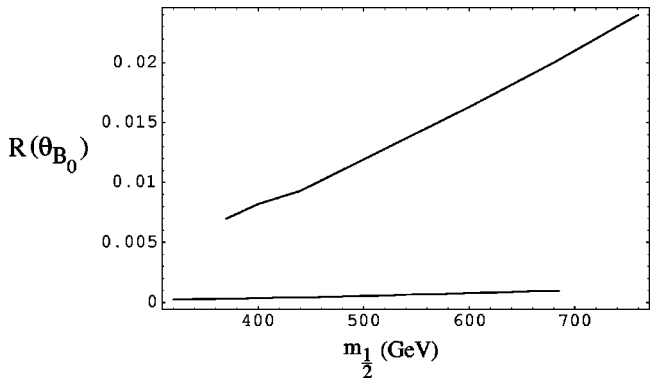

FIG. 12. $R(\theta_{B_0})$ as a function of $m_{1/2}$ for $\tan\beta=40$, $\phi_1=0.9$ for $A_0=0$ (upper curve) and $|A_0|=2m_{1/2}$, $\alpha_0=0.5$ (lower curve).

$\Delta\theta_{B_0}$ may need to be fine tuned, particularly for low $m_{1/2}$ where the SUSY mass spectrum is light. This is seen explicitly in Fig. 10 for $\tan\beta=40$, $A_0=0$ with $\phi_1=0.9$, 1.2, 1.6, 2.3, and 2.6. We see that $R(\theta_{B_0})$ decreases as ϕ_1 increases from 0.9 to 1.6 ($\cong\pi/2$) and then increases for 2.3 and 2.6 where $\pi-\phi_1$ is decreasing. [The upper bound on $m_{1/2}$ arising from the lower bound on a_μ decreases as ϕ_1 moves into the second quadrant in accord with Eqs. (20),(21).] We see that if one imposes the fine tuning constraint that $R(\theta_{B_0})>0.01$, large sections of the low $m_{1/2}$ region would be excluded, e.g., one would require $m_{1/2}>540$ GeV for $\phi_1=1.6$. The fine tuning becomes more acute at lower values of $\tan\beta$. Thus Fig. 11 shows $R(\theta_{B_0})$ as a function of $m_{1/2}$ for $\tan\beta=15$, $A_0=0$ for $\phi_1=0.9$ (upper curve) and $\phi_1=1.2$ (lower curve). Thus the fine tuning constraint would eliminate completely $\phi_1=1.2$ (and the entire region of ~ 0.4 radians around $\pi/2$) and also restricts the other values of ϕ_1. Finally, we note that increasing A_0 generally increases the amount of fine tuning needed. Thus Fig. 12 shows $R(\theta_{B_0})$ for $\tan\beta=40$, $\phi_1=0.9$ for $A_0=0$ (upper curve) and $|A_0|=2m_{1/2}$, $\alpha_0=0.5$ (lower curve). The entire $|A_0|=2m_{1/2}$ curve has $R(\theta_{B_0})<0.001$.

IV. CONCLUSIONS

We have examined here what SUSY CP violating phases are possible within the framework of SUGRA models, when the electron electric dipole moment experimental bound is imposed on the SUSY parameter space. In order to analyze this, we imposed simultaneously the accelerator bounds of the Higgs boson mass ($m_h>114$ GeV) and the $b\to s\gamma$ branching ratio, the relic density bound for neutralino cold dark matter and the recent 2.6 std deviation of the muon magnetic moment from the standard model prediction. The different experimental constraints interact with each other. Thus the Higgs boson mass and $b\to s\gamma$ constraints put lower bounds on the gaugino mass [$m_{1/2}\gtrsim(300-400)$ GeV] which puts the relic density analysis mostly in the region where stau-neutralino coannihilation occurs. This closely fixes the scalar mass m_0 in terms of $m_{1/2}$ (for fixed A_0 and $\tan\beta$). The a_μ lower bound then puts an upper bound on $m_{1/2}$. Thus the parameter space becomes highly constrained. One can estimate analytically, as was done in Sec. II, the effects of turning on the CP violating phases. In fact if d_e were zero, one could still have large CP violating phases present, with the B-ino phase ϕ_1 between 0 and 2π. The condition that a_μ be positive puts the B phase θ_B in the first and fourth quadrants with $|\theta_B|\sim 0.2$–0.4. The dependence of θ_B on $\tan\beta$ and A_0 was discussed in detail in Sec. III. It was seen that the phase ϕ_1 acts to reduce the theoretical value of a_μ by a factor $Q<1$, defined in Eqs. (20), (21), and from the experimental lower bound on a_μ this reduces the upper bound on $m_{1/2}$, limiting further the parameter space. The reduction of the upper bound on $m_{1/2}$ has several phenomenological consequences. As can be seen from Eq. (21) and Fig. 4, the effect is largest when ϕ_1 is close to π. Thus in the example of Fig. 4 when $\phi_1=3.4$, one has $m_{1/2}<515$ GeV, and θ_B is still fairly large ($\theta_B=0.14$). This can be compared to the result for $\tan\beta=40$ when all phases are zero where $m_{1/2}<790$ GeV [33]. Thus the upper bound on the gluino mass would now be 1280 GeV compared to 1960 GeV when the phases are zero. Similarly the rest of the SUSY spectrum would be significantly reduced, making the SUSY mass spectrum more accessible to accelerator discovery. Thus we find $m_{\tilde{\chi}_1^0}<220$ GeV, $m_{\tilde{\chi}_1^\pm}<421$ GeV, $m_{\tilde{e}_1}<319$ GeV, $m_{\tilde{e}_2}<446$ GeV, $m_{\tilde{\tau}_1}<225$ GeV, $m_{\tilde{\tau}_2}<445$ GeV. Hence for this example, the electroweak sector would be mostly accessible to a linear collider at 850 GeV (such as tesla [34]) though the squarks and gluinos would require the LHC.

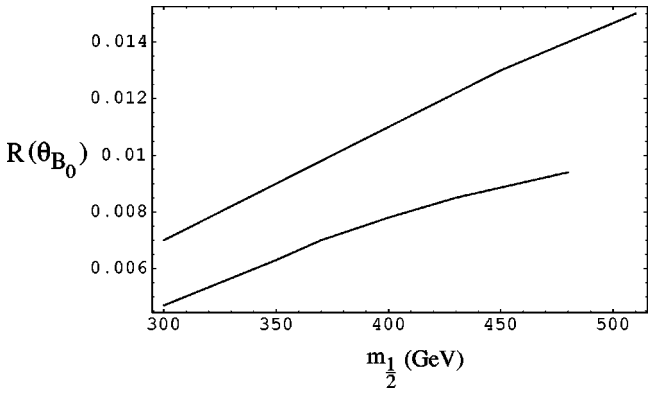

FIG. 11. $R(\theta_{B_0})$ as a function of $m_{1/2}$ for $\tan\beta=15$, $A_0=0$ for $\phi_1=0.9$ (upper curve) and $\phi_1=1.2$ (lower curve).

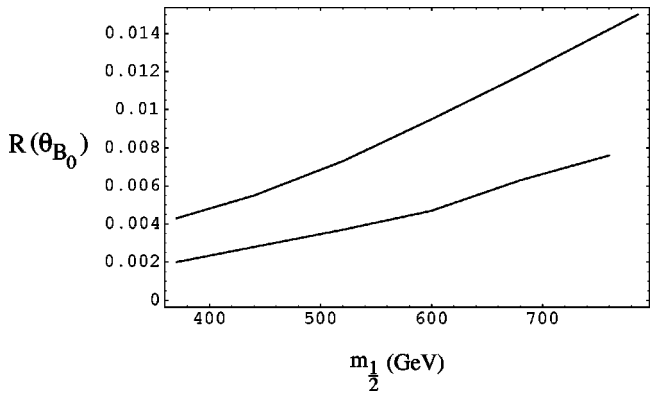

FIG. 13. $R(\theta_B)$ as a function of $m_{1/2}$ for $\tan\beta=40$, $A_0=0$, $\phi_1=0.9$ (lower curve) and $\phi_1=0.4$ (upper curve) with the current experimental bound on d_e reduced by a factor of three.

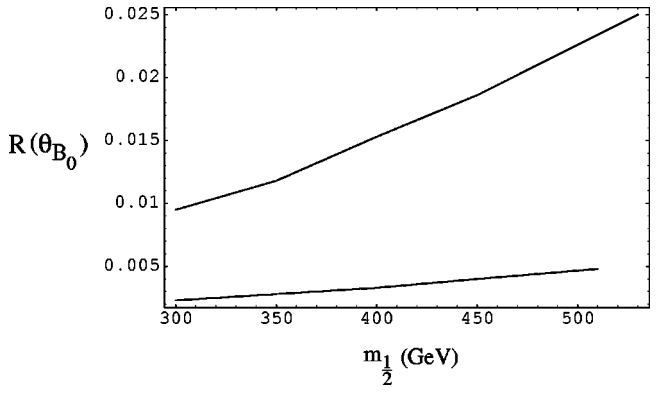

FIG. 14. $R(\theta_{B_0})$ as a function of $m_{1/2}$ for $\tan\beta=15$, $A_0=0$, $\phi_1=0.9$ (lower curve) and $\phi_1=0.3$ (upper curve) with the current experimental bound on d_e reduced by a factor of three.

A second consequence of the reduction of the upper bound on $m_{1/2}$ occurs in dark matter detection cross sections. Thus the neutralino-proton cross section is a decreasing function of $m_{1/2}$, and for example requiring $m_{1/2}<515$ GeV as above, would raise the minimum cross sections by nearly a factor of ten (to $\sim 10^{-9}$ pb) compared to the minimum cross sections without CP violating phases [15]. Future dark matter detectors would then be able more easily to scan the full SUSY parameter space. The effect of the SUSY CP violating phases should also effect the experimental accessibility of detecting the $B_s\to\mu^-\mu^+$ which also favors the large tanbeta regime. Up to now this decay has been studied in the limit of vanishing CP violating phases [35].

The relevant question, however, is whether the smallness of the experimental bound on d_e requires an unreasonable amount of fine-tuning of the phases. Using the parameter $R(\phi)=\Delta\phi/\phi_{\rm av}$, we find at the electroweak scale, both $R(\theta_B)$ and $R(\phi_1)$ are small, i.e., a few percent. However, in general $R>0.01$, and so no fine tuning below the 1% level is needed. However, at the GUT scale, this is not the case for $R(\theta_{B_0})$ for a significant part of the parameter space. Thus if we were to exclude regions where $R(\theta_{B_0})<0.01$, then for $\tan\beta=15$, $A_0=0$, ϕ_1 phases near 90° (i.e., $1.2<\phi_1<2.0$) are completely excluded (Fig. 11). The effect is reduced for higher $\tan\beta$. However, for example, for $\tan\beta=40$, $A_0=0$ the condition $R>0.01$ would eliminate $m_{1/2}<540$ GeV for $\phi_1=1.6$, and raise the lower bound on $m_{1/2}$ by a lesser amount for other values of ϕ_1 (Fig. 10). Increasing A_0 decreases the value of R, making the fine-tuning more serious, as can be seen in Fig. 12.

The fine-tuning problem is thus on the verge of becoming quite acute. The experimental bound on d_e is likely to decrease by a factor of three in the near future [29]. The effect this would have is shown in Figs. 13 and 14. Figure 13 shows $R(\theta_B)$ as a function of $m_{1/2}$ for $\tan\beta=40$, $A_0=0$, $\phi_1=0.4$ (upper curve) (corresponding to $\theta_B\simeq 0.1$) and $\phi_1=0.9$ (lower curve). The curves are what would occur if the experimental bound on d_e were reduced by a factor of three. Figure 14 shows $R(\theta_{B_0})$ as a function of $m_{1/2}$ for $\tan\beta=15$, $A_0=0$, $\phi_1=0.3$ (upper curve) (corresponding to $\theta_B\simeq 0.1$) and $\phi_1=0.9$ (lower curve), if the bound is reduced by a factor of three. $\phi_1<0.4$ in Fig. 13 and $\phi_1<0.3$ in Fig. 14 would have less fine tuning but correspond to $\theta_B<0.1$.

In a GUT theory, presumably the parameters at the GUT scale are the more fundamental ones, and fine-tuning of these parameters would presumably represent a serious problem. Of course, what level of fine-tuning one accepts is somewhat a matter of taste, and we view the criteria $R>0.01$ as merely a benchmark for consideration. However, the above results show that any significant experimental reduction of d_e would make the idea of large SUSY CP violating phases more difficult to maintain, as fine-tuning would set in even at the electroweak scale unless the SUSY masses are heavy.

Finally we mention that the lepton EDMs scale with their masses, assuming lepton universality. Thus the bound of Eq. (14) would correspond to a muon EDM bound of $8.9\times 10^{-25}e$ cm. The current bound on d_μ is $1\times 10^{-18}e$ cm (95% C.L.) [36]. However, experiments are currently being considered at Brookhaven to measure d_μ to within an accuracy of about $10^{-24}e$ cm [37], which would make the muon EDM measurements competitive with the electron measurements.

ACKNOWLEDGMENTS

This work was supported in part by National Science Foundation Grant No. PHY-0070964.

APPENDIX: DERIVATIONS

In this appendix, we calculate the leading terms in $\tan\beta$ for the complex amplitude A of Eqs. (5) and (6) needed to calculate a_μ and d_e. In order to do this, it is necessary to diagonalize the various mass matrices entering in the chargino and neutralino loops. These matrices depend on the phases ϕ_1, α_l, and $\theta=\theta_\mu+\epsilon_1+\epsilon_2$ where α_l is the phase of A_l and $\langle H_{1,2}\rangle=v_{1,2}e^{i\epsilon_{1,2}}$ where $v_{1,2}=|\langle H_{1,2}\rangle|$. Minimizing the effective potential with respect to $\epsilon_{1,2}$ determines θ in terms of θ_B, and one may then choose Higgs phases such that $\epsilon_{1,2}=0$, as was done in Eq. (1). With this choice of phases, the chargino and neutralino mass matrices are

$$M_{\tilde{\chi}^\pm}=\begin{pmatrix} \tilde{m}_2 & \sqrt{2}M_W\sin\beta \\ \sqrt{2}M_W\cos\beta & \mu \end{pmatrix} \tag{A1}$$

$$M_{\tilde{\chi}^0}=\begin{pmatrix} \tilde{m}_1 & 0 & a & b \\ 0 & \tilde{m}_2 & c & d \\ a & c & 0 & -\mu \\ b & d & -\mu & 0 \end{pmatrix} \tag{A2}$$

where $\tilde{m}_1=|\tilde{m}_1|e^{i\phi_1}$, $\mu=|\mu|e^{i\theta_\mu}$, $a=-M_Z\sin\theta_W\cos\beta$, $b=M_Z\sin\theta_W\sin\beta$, $c=-a\cot\theta_W$, $d=-b\cot\theta_W$, and $\tilde{m}_2$ has been chosen real and positive.

The slepton mass matrices have the form

$$M_{\tilde{l}}^2=\begin{pmatrix} m_{lLL}^2 & m_{lLR}^2 \\ m_{lLR}^{2*} & m_{lRR}^2 \end{pmatrix} \tag{A3}$$

where $m_{lLR}^2=m_l(A_l^*-\mu\tan\beta)$, $A_l=|A_l|e^{i\alpha_l}$, and

$$m_{lLL}^2=m_L^2+m_l^2-\frac{1}{2}(1-2\sin^2\theta_W)M_Z^2\cos 2\beta \tag{A4}$$

$$m_{lRR}^2=m_R^2+m_l^2-\sin^2\theta_W M_Z^2\cos 2\beta. \tag{A5}$$

The $m_{L,R}^2$ are obtained by running the RGE from the GUT scale to the electroweak scale [30]. In our analysis we will assume universal soft breaking of the $\tilde{\mu}$ and $\tilde{e}$ scalar masses (m_0) and universal cubic soft breaking masses (A_0) at M_G. Since m_e^2 and m_μ^2 are very small, they can be neglected at the electroweak scale, i.e., $M_{\tilde{\mu}}^2=M_{\tilde{e}}^2$.

$M_{\tilde{\chi}^0}$ is a symmetric, complex matrix and can be diagonalized by a unitary matrix X according to $M_{\tilde{\chi}^0}X=X^*M_{\tilde{\chi}^0}^{(D)}$ where

$$M_{\tilde{\chi}^0}^{(D)}=\mathrm{diag}(m_{\tilde{\chi}_1^0},m_{\tilde{\chi}_2^0},m_{\tilde{\chi}_3^0},m_{\tilde{\chi}_4^0}). \tag{A6}$$

$M_{\tilde{l}}^2$ can be diagonalized by a Hermitian matrix D with $M_{\tilde{l}}^2D=DM_{\tilde{l}}^{2(D)}$ where $M_{\tilde{l}}^{2(D)}=\mathrm{diag}(m_{\tilde{l}_1}^2,m_{\tilde{l}_2}^2)$. Finally one diagonalizes $M_{\tilde{\chi}^\pm}$ by two unitary transformations U and V according to $U^*M_{\tilde{\chi}^\pm}V^\dagger=M_{\tilde{\chi}^\pm}^{(D)}$ where $M_{\tilde{\chi}^\pm}^{(D)}=\mathrm{diag}(m_{\tilde{\chi}_1^\pm},m_{\tilde{\chi}_2^\pm})$.

The amplitude A can be divided into its chargino and neutralino parts: $A=A(\tilde{\chi}^\pm)+A(\tilde{\chi}^0)$. We follow the notation of [31] where one finds that

$$A(\tilde{\chi}^\pm)=\frac{1}{\sqrt{2}M_W\cos\beta}\sum_i\frac{1}{m_{\tilde{\chi}_i^\pm}}U_{i2}^*V_{i1}^*F_i \tag{A7}$$

and $F_i=F(m_{\tilde{\nu}}^2/m_{\tilde{\chi}_i^\pm}^2)$ with

$$F(x)=\frac{1-3x}{(1-x)^2}-\frac{2x^2\ln x}{(1-x)^3}. \tag{A8}$$

Similarly

$$A(\tilde{\chi}^0)=\frac{1}{m_l}\sum_{k,j}\frac{1}{m_{\tilde{\chi}_j^0}}\left(\eta_j^kG_{kj}+\frac{m_l}{6}X_j^kH_{kj}\right) \tag{A9}$$

where

$$\eta_j^k=-\left[\frac{1}{\sqrt{2}}(\tan\theta_WX_{1j}+X_{2j})D_{1k}^*-\kappa_lX_{3j}D_{2k}^*\right]\times[\sqrt{2}\tan\theta_WX_{1j}D_{2k}+\kappa_lX_{3j}D_{1k}], \tag{A10}$$

$$X_j^k=\frac{1}{2}\tan^2\theta_W|X_{1j}|^2(|D_{1k}|^2+4|D_{2k}|^2)+\frac{1}{2}|X_{2j}|^2|D_{1k}|^2+\tan\theta_W|D_{1k}|^2X_{1j}X_{2j}^*+O(m_l) \tag{A11}$$

and $\kappa_l=m_l/(\sqrt{2}M_W\cos\beta)$. The loop integrals are $G_{kj}=G(m_{\tilde{l}_k}^2/m_{\tilde{\chi}_j^0}^2)$, $H_{kj}=H(m_{\tilde{l}_k}^2/m_{\tilde{\chi}_j^0}^2)$ where

$$G(x)=\frac{1+x}{(1-x)^2}+\frac{2x}{(1-x)^3}\ln x \tag{A12}$$

$$H(x)=\frac{2+5x-x^2}{(1-x)^3}+\frac{6x}{(1-x)^4}\ln x. \tag{A13}$$

We need only keep the terms in A independent of m_l and thus can neglect the $O(m_l)$ terms in Eq. (A11). (Actually, η_l^k begins linearly in m_l.)

We are interested in calculating only the leading terms in $\tan\beta$. We will also do this in the limit $M_W^2/|\mu|^2\ll 1$ and $M_W^2/|\tilde{m}_i|^2\ll 1$ (which is valid for most of the MSUGRA parameter space). In that case one has [32]

$$m_{\tilde{\chi}_1^0}\cong|\tilde{m}_1|;\quad m_{\tilde{\chi}_2^0}\cong m_{\tilde{\chi}_1^\pm}\cong\tilde{m}_2;\quad m_{\tilde{\chi}_{3,4}^0}\cong m_{\tilde{\chi}_2^\pm}\cong|\mu|. \tag{A14}$$

We consider first the calculation of $A(\tilde{\chi}^\pm)$. Since V diagonalizes $M_{\tilde{\chi}^\pm}^\dagger M_{\tilde{\chi}^\pm}$ and U^* diagonalizes $M_{\tilde{\chi}^\pm}M_{\tilde{\chi}^\pm}^\dagger$ one finds for the leading terms

$$U_{12}^*\cong-\frac{1}{\mu}\sqrt{2}M_W\sin\beta\frac{|\mu|^2}{|\mu|^2-\tilde{m}_2^2}U_{11}^* \tag{A15}$$

$$V_{21}\cong\frac{1}{\tilde{m}_2}\sqrt{2}M_W\sin\beta\frac{\tilde{m}_2^2}{|\mu|^2-\tilde{m}_2^2}V_{22}. \tag{A16}$$

With an appropriate choice of phases one has to lowest order $U_{11}\cong 1\cong U_{22}$, $V_{11}\cong 1$, and

$$V_{22}\cong e^{i\theta_\mu}. \tag{A17}$$

Hence inserting into Eq. (A7) gives

$$A(\tilde{\chi}^{\pm})=-\frac{\tan\beta}{\tilde{m}_2|\mu|}e^{-i\theta_\mu}\left[\frac{|\mu|^2}{|\mu|^2-\tilde{m}_2^2}F_1-\frac{\tilde{m}_2^2}{|\mu|^2-\tilde{m}_2^2}F_2\right]. \tag{A18}$$

To calculate the leading terms of $A(\tilde{\chi}^0)$ it is useful to first note the size of the matrix elements X_{ij}. Thus to zeroth order in M_Z

$$X_{11}\cong e^{-(i/2)\phi_1},\quad X_{22}\cong 1 \tag{A19}$$

$$X_{33}\cong -X_{43}\cong\frac{1}{\sqrt{2}}e^{-(i/2)\theta_\mu},\quad X_{34}\cong X_{44}\cong e^{\pi i/2}X_{33}. \tag{A20}$$

Also one has X_{12}, X_{21} are $O(M_Z^2)$ (and hence negligible) while the remaining components are $O(M_Z)$. To lowest order, the slepton mass eigenvalues are $m_{\tilde{l}_1}^2\cong m_{lRR}^2$, $m_{\tilde{l}_2}^2\cong m_{lLL}^2$, and the D matrix has the form $D_{12}\cong 1\cong D_{21}$ and

$$D_{11}\cong-\frac{m_l(A_l^*-\mu\tan\beta)}{m_{\tilde{l}_2}^2-m_{\tilde{l}_1}^2}\cong -D_{22}^*. \tag{A21}$$

To illustrate the calculation of $A(\tilde{\chi}^0)$ we consider the leading term when $k=1=j$. From Eq. (A10), two terms contribute to η_1^1 for large $\tan\beta$:

$$\eta_1^1=-\left(\frac{1}{\sqrt{2}}\tan\theta_W X_{11}D_{11}^*\right)(\sqrt{2}\tan\theta_W X_{11}D_{21})+(\kappa_l X_{31}D_{21}^*)\times(\sqrt{2}\tan\theta_W X_{11}D_{21}) \tag{A22}$$

which evaluates to

$$\eta_1^1=-\frac{m_l\tan^2\theta_W\tan\beta}{|\mu|}\left[\frac{|\mu|^2}{m_{\tilde{l}_2}^2-m_{\tilde{l}_1}^2}-\frac{|\mu|^2}{|\mu|^2-|\tilde{m}_1|^2}\right]\times e^{-i(\theta_\mu+\phi_1)} \tag{A23}$$

where we have used

$$X_{31}\cong\frac{M_Z\sin\theta_W\sin\beta}{\mu}\frac{|\mu|^2}{|\mu|^2-|\tilde{m}_1|^2}X_{11}. \tag{A24}$$

[Note that η_1^1 is linear in m_l and hence Eq. (A9) is not singular as $m_l\to 0$.] In a similar fashion one can obtain all the leading terms in Eq. (A9). [The X_j^k terms of Eq. (A11) do not contribute.] The total answer is

$$\begin{aligned}A(\tilde{\chi}^0)\cong&-\frac{\tan^2\theta_W\tan\beta}{|\tilde{m}_1||\mu|}\left[\left\{\left(\frac{|\mu|^2}{m_{\tilde{l}_2}^2-m_{\tilde{l}_1}^2}-\frac{|\mu|^2}{|\mu|^2-|\tilde{m}_1|^2}\right)G_{11}\right.\right.\\&\left.\left.-\left(\frac{|\mu|^2}{m_{\tilde{l}_2}^2-m_{\tilde{l}_1}^2}-\frac{1}{2}\frac{|\mu|^2}{|\mu|^2-|\tilde{m}_1|^2}\right)G_{21}\right\}e^{-i(\theta_\mu+\phi_1)}\right.\\&-\frac{1}{2}\frac{1}{\tan^2\theta_W}\frac{|\mu|^2}{|\mu|^2-\tilde{m}_2^2}\left(\frac{|\tilde{m}_1|}{\tilde{m}_2}G_{22}-\frac{1}{2}\frac{|\tilde{m}_1|\tilde{m}_2}{|\mu|^2}G_{23}\right)\\&\left.\times e^{-i\theta_\mu}+\frac{1}{4}\frac{1}{\tan^2\theta_W}\frac{|\tilde{m}_1|}{|\mu|}\frac{|\mu|^2}{|\mu|^2-\tilde{m}_2^2}G_{23}\right].\end{aligned} \tag{A25}$$

We note that a large amount of cancellation occurs in this regime: terms proportional to G_{24} have all canceled with part of the G_{23} terms, and the total G_{14} contribution cancels with the G_{13} terms. Note also that the $A(\tilde{\chi}^0)$ depends separately on two phase combinations: $\theta_\mu+\phi_1$ and θ_μ, though terms depending on $\theta_\mu+\phi_1$ are generally larger.

[1] See, e.g., BaBar Collaboration, J. Beringer *et al.*, hep-ex/0105073; P. Chang for the BELLE Collaboration, Nucl. Phys. **A684**, 704 (2001); for a review, see T. Hurth *et al.*, J. Phys. G **27**, 1277 (2001).

[2] T. Falk and K. Olive, Phys. Lett. B **375**, 196 (1996); T. Ibrahim and P. Nath, *ibid.* **418**, 98 (1998); Phys. Rev. D **57**, 478 (1998); **58**, 019901(E) (1998); **60**, 079903(E) (1999); **60**, 119901(E) (1999).

[3] T. Falk and K. Olive, Phys. Lett. B **439**, 71 (1998); M. Brhlik, G. Good, and G. Kane, Phys. Rev. D **59**, 115004 (1999); M. Brhlik, L. Everett, G. Kane, and J. Lykken, Phys. Rev. Lett. **83**, 2124 (1999); Phys. Rev. D **62**, 035005 (2000); A. Bartl, T. Gajdosik, W. Porod, P. Stockinger, and H. Stremnitzer, *ibid.* **60**, 073003 (1999); S. Pokorski, J. Rosiek, and C. A. Savoy, Nucl. Phys. **B570**, 81 (2000).

[4] E. Accomando, R. Arnowitt, and B. Dutta, Phys. Rev. D **61**, 075010 (2000).

[5] T. Falk, K. Olive, M. Pospelov, and R. Roiban, Nucl. Phys. **B560**, 3 (1999).

[6] V. Barger, T. Falk, T. Han, J. Jiang, T. Li, and T. Plehn, Phys. Rev. D **64**, 056007 (2001); S. Abel, S. Khalil, and O. Lebedev, Nucl. Phys. **B605**, 151 (2001).

[7] Muon (g-2) Collaboration, H. N. Brown *et al.*, Phys. Rev. Lett. **86**, 2227 (2001).

[8] J. Feng and K. Matchev, Phys. Rev. Lett. **86**, 3480 (2001); U. Chattopadhyay and P. Nath, *ibid.* **86**, 5854 (2001); S. Komine, T. Moroi, and M. Yamaguchi, Phys. Lett. B **506**, 93 (2001); **507**, 224 (2001); T. Ibrahim, U. Chattopadhyay, and P. Nath, Phys. Rev. D **64**, 016010 (2001); J. Ellis, D. V. Nanopoulos, and K. A. Olive, Phys. Lett. B **508**, 65 (2001); R. Arnowitt, B. Dutta, B. Hu, and Y. Santoso, *ibid.* **505**, 177 (2001); S. Martin and J. Wells, Phys. Rev. D **64**, 035003 (2001); H. Baer, C. Balazs, J. Ferrandis, and X. Tata, *ibid.* **64**, 035004 (2001); F. Richard, hep-ph/0104106; D. Carvalho, J. Ellis, M. Gomez,

and S. Lola, hep-ph/0103256; S. Baek, T. Goto, Y. Okada, and K. Okumura, hep-ph/0104146; Y. Kim and M. Nojiri, hep-ph/0104258.

[9] T. Ibrahim, U. Chattopadhyay, and P. Nath, Phys. Rev. D **64**, 016010 (2001).

[10] A. H. Chamseddine, R. Arnowitt, and P. Nath, Phys. Rev. Lett. **49**, 970 (1982); R. Barbieri, S. Ferrara, and C. A. Savoy, Phys. Lett. **119B**, 343 (1982); L. Hall, J. Lykken, and S. Weinberg, Phys. Rev. D **27**, 2359 (1983); P. Nath, R. Arnowitt, and A. H. Chamseddine, Nucl. Phys. **B227**, 121 (1983).

[11] L. Randall and R. Sundrum, Nucl. Phys. **B557**, 79 (1999); G. Giudice, M. Luty, H. Murayama, and R. Rattazzi, J. High Energy Phys. **12**, 027 (1998).

[12] M. Dine and A. Nelson, Phys. Rev. D **48**, 1277 (1993); M. Dine, A. Nelson, and Y. Shirman, *ibid.* **51**, 1362 (1995); M. Dine, A. Nelson, Y. Nir, and Y. Shirman, *ibid.* **53**, 2658 (1996); S. Dimopoulos, S. Thomas, and J. Wells, Nucl. Phys. **B488**, 39 (1997); J. Bagger, K. Matchev, D. Pierce, and R-j. Zhang, Phys. Rev. D **55**, 3188 (1997); D. Dicus, B. Dutta, and S. Nandi, Phys. Rev. Lett. **78**, 3055 (1997); for a review, see G. Giudice and R. Rattazzi, Phys. Rep. **322**, 419 (1999).

[13] J. Feng and K. Matchev, in Ref. [8]; K. Choi, K. Hwang, S. K. Kang, K. Y. Lee, and W. Y. Song, Phys. Rev. D **64**, 055001 (2001).

[14] T. Han and R. Hempfling, Phys. Lett. B **415**, 161 (1997).

[15] R. Arnowitt, B. Dutta, and Y. Santoso, Nucl. Phys. **B606**, 59 (2001).

[16] J Ellis, T. Falk, G. Ganis, K. Olive, and M. Srednicki, Phys. Lett. B **510**, 236 (2001); M. Gomez and J. Vergados, *ibid.* **512**, 252 (2001); M. Gomez, G. Lazarides, and C. Pallis, Phys. Rev. D **61**, 123512 (2000); Phys. Lett. B **487**, 313 (2000); J. Ellis, T. Falk, and K. Olive, *ibid.* **444**, 367 (1998); J. Ellis, T. Falk, K. Olive, and M. Srednicki, Astropart. Phys. **13**, 181 (2000); **15**, 413(E) (2001).

[17] D. A. Kosower, L. M. Krauss, and N. Sakai, Phys. Lett. **133B**, 305 (1983); T. C. Yuan, R. Arnowitt, A. H. Chamseddine, and P. Nath, Z. Phys. C **26**, 407 (1984).

[18] J. L. Lopez, D. V. Nanopoulos, and X. Wang, Phys. Rev. D **49**, 366 (1994); U. Chattopadhyay and P. Nath, *ibid.* **53**, 1648 (1996); T. Moroi, *ibid.* **53**, 6565 (1996); **56**, 4424(E) (1997); M. Carena, G. F. Giudice, and C. E. M. Wagner, Phys. Lett. B **390**, 234 (1997); T. Goto, Y. Okada, and Y. Shimizu, hep-ph/9908499; T. Blazek, hep-ph/9912460; G. C. Cho, K. Hagiwara, and M. Hayakawa, Phys. Lett. B **478**, 231 (2000); T. Ibrahim and P. Nath, Phys. Rev. D **62**, 015004 (2000); M. Drees, Y. Kim, T. Kobayashi, and M. Nojiri, *ibid.* **63**, 115009 (2001).

[19] D. Demir, Phys. Rev. D **60**, 055006 (1999).

[20] M. Pospelov and A. Ritz, Phys. Rev. D **63**, 073015 (2001); M. Hecht, C. Roberts, and S. Schmidt, Phys. Rev. C **64**, 025204 (2001).

[21] E. D. Commins *et al.*, Phys. Rev. A **50**, 2960 (1994).

[22] P. Igo-Kimenes, Talk presented at ICHEP 2000, Osaka, Japan, 2000.

[23] M. Alam *et al.*, Phys. Rev. Lett. **74**, 2885 (1995).

[24] G. Degrassi, P. Gambino, and G. Giudice, J. High Energy Phys. **12**, 009 (2000); M. Carena, D. Garcia, U. Nierste, and C. Wagner, Phys. Lett. B **499**, 141 (2001).

[25] R. Rattazi and U. Sarid, Phys. Rev. D **53**, 1553 (1996); M. Carena, M. Olechowski, S. Pokorski, and C. Wagner, Nucl. Phys. **B426**, 269 (1994).

[26] C. Netterfield *et al.*, astro-ph/0104460.

[27] A. T. Lee *et al.*, astro-ph/0104459.

[28] R. Garisto and J. Wells, Phys. Rev. D **55**, 1611 (1997).

[29] David DeMille (private communication).

[30] L. Ibanez and C. Lopez, Nucl. Phys. **B233**, 511 (1984).

[31] T. Ibrahim and P. Nath, Phys. Rev. D **62**, 015004 (2000).

[32] R. Arnowitt and P. Nath, Phys. Rev. Lett. **69**, 725 (1992).

[33] R. Arnowitt, B. Dutta, B. Hu, and Y. Santoso, in Ref. [8].

[34] R. Brinkmann, talk at Snowmass 2001, 2001.

[35] A. Dedes, H. K. Dreiner, and U. Nierste, hep-ph/0108037.

[36] J. Bailey *et al.*, Nucl. Phys. **B150**, 1 (1979).

[37] Y. K. Semertzidis *et al.*, hep-ph/0012087.